

# Circular Polarization Selective Metamaterial Absorber in Terahertz Frequency Range

Danka B. Stojanović , Goran Gligorić, Petra P. Beličev, Milivoj R. Belić , and Ljupčo Hadžievski

**Abstract**—In this article, we propose a chiral metamaterial absorber based on four rotated twisted closed ring resonators operative in terahertz frequency range. The resonant features are analyzed by electric field amplitude distributions, and surface currents flow generated by the interaction of circularly polarized waves with the chiral structure. The highest field amplitudes at the fundamental resonance are obtained at the gap region of the resonator. Therefore, the efficiency of the proposed absorber is determined through response of absorption spectrum around this resonance with variation of geometrical parameters of the structure. Significant increase of absorption of the left circularly polarized light is obtained with variation of the period size of structure. Consequently, huge circular dichroism, and near-unity polarization selective absorption have been provided. This makes the proposed chiral structure a good candidate for designing circular polarization selective absorber.

**Index Terms**—Chirality, circularly polarized waves, metamaterial absorbers, terahertz range.

## I. INTRODUCTION

IN RECENT years, there is a growing interest in designing a different components operating at terahertz (THz) frequencies for construction of systems required for THz communications and sensing [1], [2]. It is expected that good detection abilities of metamaterial based sensing technology will provide a wide range of applications in the near future as electromagnetic absorbers, filters and sensors [3]–[8]. The special attention has been focused on resonant metamaterial absorbers which rely on achieving near-unity absorption at narrow range around resonant frequency [9]–[11].

In particular, our interest is in chiral metamaterials as they enable different coupling with left (LCP) and right (RCP) circularly polarized waves [12], [13] which provides them as suitable

candidate for circular polarization selective absorbers [14]. Actually, chirality is a feature of an object which lacks any mirror symmetry plane. In the interaction with circularly polarized light, chiral medium enables an appearance of chiroptical effects such as optical activity and circular dichroism [15], [16]. Accordingly, properties of chiral metamaterials to enable circular polarization selection and control propagation of THz wave are very important for applications in circular dichroism spectroscopy, holographic imaging and biomolecule detection [17], [18]. For example, circular dichroism spectroscopy can be used for the identification of chiral molecules at THz frequencies but the problem is lack of light modulators of circularly polarized waves. Therefore, development of these components is of great importance [19], [20].

To this end, intensive efforts have been made to realize chirality selective metamaterial absorbers in microwave range [14], [21], at IR frequencies [22]–[24], as well as in visible range [25]. By using “L” shaped metamaterial, absorption up to 93.2% for LCP and 8.4% for RCP waves at GHz range has been reported in [21]. Furthermore, at near-IR frequencies, structure based on chiral “Z” shaped resonators acts as a perfect LCP light absorber at the resonant frequency reflecting nearly 95% of RCP light [23]. Even higher value of absorption is achieved in mid-IR region for bi-layer metamaterial structure giving absorption of 99.3% for RCP wave (for LCP wave absorption of 5.3% was obtained at the same resonance) [22]. However, there is also a need to selectively control the states of circular polarization at THz frequencies. Until now, only a few investigations of chiral absorbers in THz frequency range were carried out, taking into account both, broadband and frequency selective structures [26], [27].

In this paper, we present chiral metamaterial based on four rotated twisted closed ring resonators (TCRRs) and demonstrate its performances as appropriate for design of THz chiral absorbers. The study was done numerically by using finite-element method. Our focus is on the interaction of the chiral structure with circularly polarized light and calculation of circular dichroism, defined as difference of absorption coefficients of LCP and RCP waves. A key step is a proper choice of dielectric and conducting materials for designing efficient THz devices. Therefore, we carefully choose low-loss dielectric which surrounded TCRRs made of gold [28], [29]. The other critical issue for obtaining perfect absorption is the geometry of metamaterial [30], [31]. In particular, geometrical parameters have a significant influence on chiral effects, circular dichroism and optical activity [32], [33]. Hence, we analyze coupling effects through the impact

Manuscript received January 28, 2020; revised July 21, 2020 and September 12, 2020; accepted September 12, 2020. Date of publication September 18, 2020; date of current version October 14, 2020. (Corresponding author: Danka B. Stojanović.)

Danka B. Stojanović is with the Department of Atomic Physics, VINČA Institute of Nuclear Sciences, National Institute of Republic of Serbia, University of Belgrade, 11 000 Belgrade, Serbia, and with Texas A&M University at Qatar, Doha, Qatar (e-mail: dankas@vin.bg.ac.rs).

Goran Gligorić, Petra P. Beličev, and Ljupčo Hadžievski are with the Department of Atomic Physics, VINČA Institute of Nuclear Sciences, National Institute of Republic of Serbia, University of Belgrade, 11 000 Belgrade, Serbia (e-mail: goran79@vin.bg.ac.rs; petrab@vin.bg.ac.rs; ljupcoh@vin.bg.ac.rs).

Milivoj R. Belić is with Texas A&M University at Qatar, Doha, Qatar (e-mail: milivoj.belic@qatar.tamu.edu).

Color versions of one or more of the figures in this article are available online at <https://ieeexplore.ieee.org>.

Digital Object Identifier 10.1109/JSTQE.2020.3024570

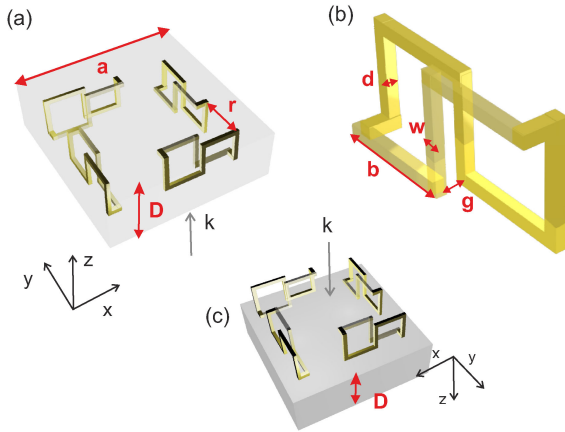


Fig. 1. (a) Unit cell of TCRR based chiral metamaterial, (b) illustration of single TCRR with geometrical parameters, (c) and unit cell of TCRR structure placed on the top of the dielectric substrate. Wave vector of incident field is denoted with  $k$ .

of different geometric parameters on the change of absorption features of the metamaterial. Also, the nature of resonant peaks is investigated via absorption spectra parameters (quality factor and FWHM), electric fields distributions and current flows. Quality factor (Q) of the resonance is a sensitivity measure of the device [11], [34], while FWHM describes the losses. Both parameters play important role in efficiency estimation of the metamaterial absorber. Furthermore, it has been reported that the period of the unit cell plays the most significant role in determination of resonance behaviour [35]. In general, our goal is oriented towards the improvement of the geometry of proposed chiral metamaterial based on TCRRs in order to obtain near-unity, circular polarization selective absorption.

## II. DESIGN OF CHIRAL METAMATERIAL

The unit cell of chiral metamaterial comprises four rotated TCRRs (depicted in Fig. 1(a)) which are periodically arranged in  $x, y$  directions of the dielectric slab. The geometry of TCRR resonator is compact and chiral as the one proposed in ref. [36](see Fig. 1(b)), but the mutual orientation is different (Figs. 1(a) and (c)). TCRR resonator is three-dimensional element obtained by twisting the ring resonator around the central part. One way to obtain this resonant element is connection of one S and zig-zag element. In the scope of practical realization, this kind of three dimensional structure is somewhat delicate. Results published in [37], [38] indicate possible realization with a three-level photolithography technique providing precise alignment of layers. Especially the structure resulting from the second step of fabrication process of the fractional-screw-like configuration depicted in Fig. 1 in [38], resembles to TCRR. With smaller modifications in design and dimensions resizing, fabrication of twisted elements should be feasible. However, this type of fabrication process is more suitable for the on-top of the substrate approach. Structures with dielectric substrates can provide mechanical robustness and stability to metallic structure, and at the same time, maintain or even enhance overall performance of the metamaterial [39], [40], thus enabling easier fabrication procedure. Therefore, we additionally examined the

case when TCRR structure is placed on the top of dielectric substrate (depicted in Fig. 1(c)). Furthermore, with quick and robust spectral THz measurements [41], the proposed structure can be characterized.

We have performed numerical simulations by using the following geometric parameters: dielectric thickness  $D = 12 \mu\text{m}$ , wire thickness  $d = 1 \mu\text{m}$ , cross-area width  $w = 2 \mu\text{m}$ , cross-area height  $g = 1 \mu\text{m}$  and length of each arm of the ring  $b = 6 \mu\text{m}$ . Parameter  $r = 2 \mu\text{m}$  is the distance in between each TCRR in the unit cell which size is defined by parameter  $a$ . For our study, we varied parameter  $w$  in the range of  $1\text{--}3 \mu\text{m}$ , as well as  $a$  from  $20 \mu\text{m}$  to  $50 \mu\text{m}$  and  $r$  from 2 to  $10 \mu\text{m}$ .

## III. NUMERICAL SIMULATIONS

Numerical simulations are carried out by solving the Maxwell equations in the frequency domain using the finite-element method implemented in the Comsol Multiphysics software. The calculation is performed for the case of normal incidence of light on the chiral metamaterial slab placed in the air. Wave vector  $k$  is aligned with the positive  $z$ -axis direction. It is assumed that the slab is made of gold elements immersed in cyclic olefin copolymer (COC) with index of refraction  $n = 1.52 + 0.0008i$  [42]. Due to significantly low loss with the absorption coefficient less than  $1.5 \text{ cm}^{-1}$  (at 4 THz) and stable index of refraction within THz range, TOPAS (type of COC) has already found applications in THz technology [43], [44]. We did additional calculations in the case of substrate made of TOPAS dielectric. An alternative dielectric for practical realization of the structure could be Zeonor. The structure with Zeonor has very similar absorption spectra around 4 THz as TOPAS having advantage of lower cost [45]. We assumed that resonant elements are made of gold as it exhibits high conductivity, small nonradiative loss and good mechanical stability [46]. As the penetration depth of light into gold typical for examined frequency range is around 30 nm, we assumed that it is negligible in comparison with the thickness of the wire of which the elements are composed ( $d = 1 \mu\text{m}$ ). Therefore, we apply the impedance boundary conditions on the surface between gold TCRRs and surrounding media. The permittivity of gold elements is described by the Drude model:

$$\varepsilon_g(\omega) = 1 - \frac{\omega_p^2}{\omega(\omega + i\omega_c)}, \quad (1)$$

where  $\omega_p = 137.15 \times 10^{14} \text{ rad/s}$ ,  $\omega_c = 40.5 \times 10^{12} \text{ rad/s}$  are plasma and collision frequency [47], respectively, while  $\omega$  represents the angular frequency of the incident wave. In all simulations, the amplitude of the incident electric field is fixed and equals  $1 \text{ V/m}$ .

As we are considering periodic structure, we applied periodic boundary conditions (Floquet periodicity) to relate side boundaries of every unit cell. For description of incident circularly polarized electric field  $E_i$  we used port boundary conditions in the following form:

$$E_{i\sigma} = E_0 \begin{bmatrix} 1 \\ i\sigma \end{bmatrix} e^{ikz} \quad (2)$$

where  $E_0 = 1 \text{ V/m}$ ,  $k$  is the wave vector in vacuum and  $\sigma = \pm$ . Sign plus stands for RCP waves while minus sign is for LCP

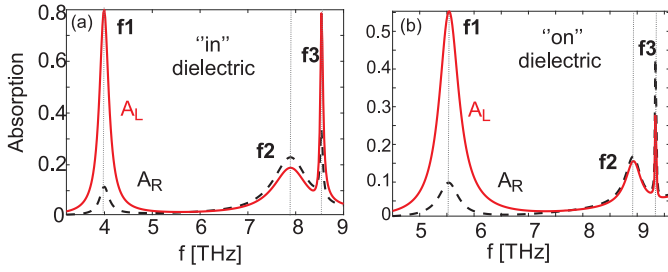


Fig. 2. Absorption spectra with three resonances for the case of incident RCP ( $A_R$  - dash line) and LCP ( $A_L$  - solid line) waves for the TCRRs structure ( $a = 25 \mu\text{m}$ ): (a) embedded in dielectric (Fig. 1(a)) and (b) placed on the top of the dielectric substrate (Fig. 1(c)).

waves. Hence, RCP electric field vector rotates counterclockwise while LCP rotates clockwise.

#### IV. RESULTS AND DISCUSSION

Fig. 2 presents absorption spectra as functions of frequency of the incident RCP and LCP waves. The absorption can be derived from the scattering coefficients:

$$A_L = 1 - |R_{RL}|^2 - |R_{LL}|^2 - |T_{LL}|^2 - |T_{RL}|^2, \quad (3)$$

$$A_R = 1 - |R_{LR}|^2 - |R_{RR}|^2 - |T_{RR}|^2 - |T_{LR}|^2, \quad (4)$$

where R and T are reflection and transmission coefficients of left (L) and right (R) circularly polarized waves. Cross-polarized coefficients in transmission and co-polarized in reflection are negligible. On the other hand, cross-polarized reflections are equal  $R_{LR} = R_{RL} = R$  due to the four folded geometry of the unit cell. Detailed calculation of scattering coefficients is presented later in the paper (spectra can be seen in Fig. 4(c)).

Firstly, we consider the case with  $a = 25 \mu\text{m}$  and TCRR structure embedded in dielectric, as depicted in Fig. 2(a). Three resonant peaks can be distinguished in the spectra up to 9 THz. First (fundamental) resonance is at  $f_1 = 3.99$  THz while second and third one are very close, at  $f_2 = 7.9$  THz and  $f_3 = 8.54$  THz, respectively. Actually, the last two are hybridized resonances [48] and there is a small value of circular dichroism ( $\text{CD} = A_L - A_R$ ) at these frequencies. On the other hand, CD has high value at  $f_1$  which is a consequence of much larger value of LCP wave absorption,  $A_L = 80\%$ . This fact indicates that at this resonance, structure has potential for applications such as circular polarization selective absorbers. In addition, we present the case in which dielectric is considered as a substrate with the same thickness as in previous case (Fig. 2(b)). Now, resonances are shifted towards higher frequencies ( $f_1 = 5.54$  THz,  $f_2 = 8.9$  THz,  $f_3 = 9.3$  THz) and maximum value of CD at the first one is 55%. These changes in spectra originate from difference of the medium surrounding the metal structure which modifies the coupling of electromagnetic waves. As a result, reduced values of the absorption maxima with peak width broadening can be noticed. Due to this lower performance of the structure with dielectric substrate, we continue our investigation for the case of the structure immersed in dielectric.

In order to gain better understanding of electromagnetic wave coupling at these resonances, we analyze distribution of the electric field amplitude  $|E|$ . As expected from the absorption results, LCP wave exhibits stronger electric field enhancement than RCP wave at resonances  $f_1$  and  $f_3$ . In Fig. 3(a) it is shown that the electric field of fundamental LC resonance,  $f_1$ , is mainly localized in the gap region, as it was the case for the structure with the unit cell based on single TCRR [36]. Consequently, due to capacitive behaviour of the structure at this frequency, there is a very weak current flow in the gap region. At the second resonance, the electric field has much lower values and the maximum is on the side parts of TCRR. Third resonance, which is overlapped with the second one, is characterized with maximum values of  $|E|$  located on the opposite sides of TCRRs than in the case of resonance  $f_2$ . Furthermore, in Fig. 3(b) are schematically presented surface current flows at these two resonances. At resonance  $f_2$ , antiparallel current flow lines can be seen in the gap region while parallel ones can be noticed at the third resonance. They are the consequence of electric dipoles and quadrupoles at these resonances [48]. Also, it is evident that depending on type of circular polarization of the incident wave, directions of surface currents change in the gap region.

Now we focus on the absorption analyses at resonance  $f_1$  due to significant CD observed in Fig. 2(a). In order to further determine the operation possibilities of this metamaterial, we investigate the impact of the periodicity (unit cell dimension -  $a$ ) on the absorption peak value. Comparing the resonances obtained with the change of periodicity, we observe two effects. First one is a small shift of resonant frequency to lower frequencies with the increase of period, and the other one is variation of the absorption peak value (Fig. 4(a)). It can be noticed that there is a significant dependance of absorption amplitude of LCP wave on period size and it becomes higher as  $a$  increases. Interestingly, the highest value of  $A_L$  obtained for  $a = 40 \mu\text{m}$  equals 92.1% while for  $a > 40 \mu\text{m}$  it decreases again down to 87%. On the other hand,  $A_R$  has lower values with the increase of  $a$  and the minimum peak value is around 6.5% for  $a = 50 \mu\text{m}$ , while for  $a = 40 \mu\text{m}$  it is  $A_R = 7.8\%$  (Fig. 4(b)). This is a significant result as CD reached a value 84.3% which is higher than the one obtained by using T-shaped structure [27]. For that structure, the absorbance for LCP wave was 91% and 24%, while the one for RCP wave was 15% and 97% at 1.91 THz and 2.91 THz, respectively. This means that CD is equal to 76% when the structure is considered as LCP absorber and 73% for RCP absorber. As in our case, first resonance is frequency selective, while at second one, selectivity is lost (widened and non-Lorentzian peak can be observed). Additionally, our structure provides three resonant frequencies in absorption spectra which can be tuned by variation of geometrical parameters. Furthermore, the value of CD is much higher in this study than in our previous investigation associated with TCRR based structure [36]. There are two main reasons for this result. First one comes from the C4 symmetry of the unit cell. Here, the bianisotropy effects are eliminated and the coupling between TCRR becomes more efficient. The other one is related with the optimal unit cell period which increased the absorption peak and consequently made the structure more functional as a chiral absorber at THz frequencies. From Fig. 4(c)



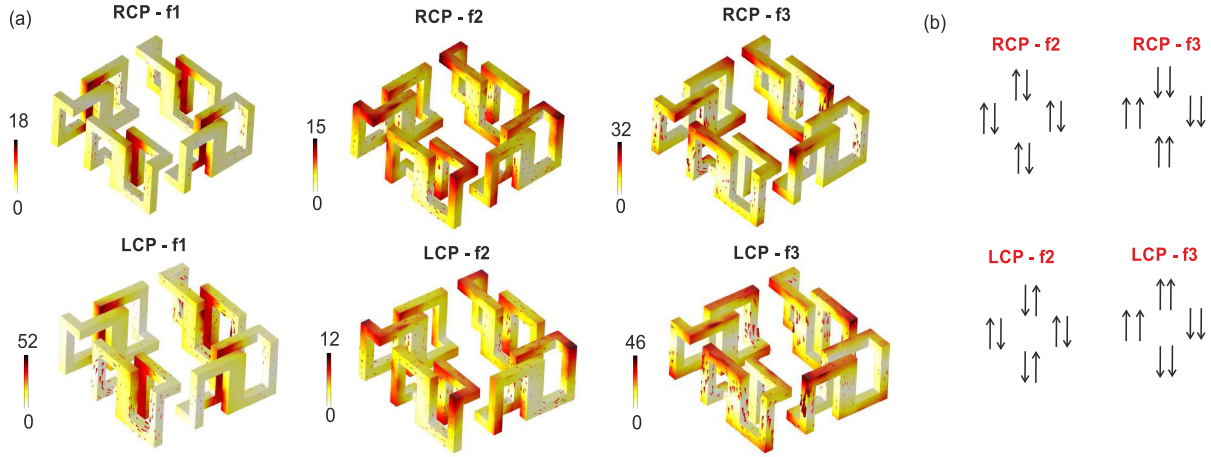


Fig. 3. (a) Electric field amplitude  $|E|$  distribution on the surface of TCRRs at  $f_1$ ,  $f_2$ , and  $f_3$  and (b) surface current flows in the gap region of each TCRR at the second and third resonance ( $a = 25 \mu\text{m}$ ). Units of maximum values of  $|E|$  at the colorbars are in V/m.

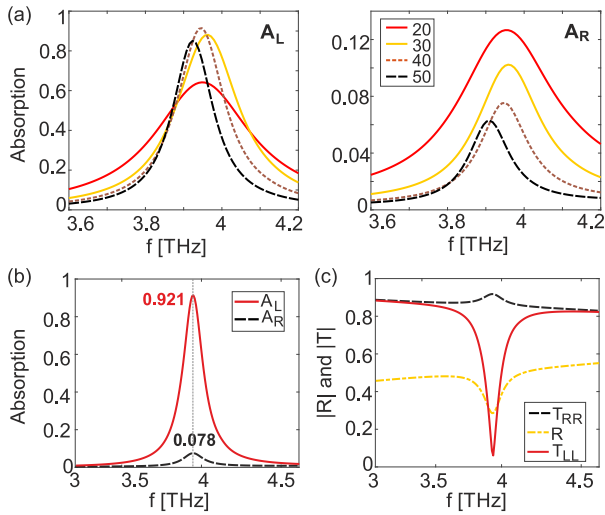


Fig. 4. (a) Absorption spectra of incident LCP (left plot) and RCP (right plot) waves with the change of period of the structure (legend is in  $\mu\text{m}$ ); (b) Absorption of LCP and RCP waves ( $a = 40 \mu\text{m}$ ). (c) Scattering coefficients of incident LCP and RCP waves ( $a = 40 \mu\text{m}$ ).

can be seen that the resonant transmission of LCP wave equals  $T_{LL} = 0.04$ , while of RCP wave is  $T_{RR} = 0.92$ . The value of  $T_{RR}$  is almost constant around first resonance indicating weak interaction of RCP wave with the structure. Reflection coefficient has the same values in both cases,  $R = 0.27$ , which is explained at the beginning of this section.

Next, we examine Q factor of the resonance by considering the absorption peak. Presuming that absorption spectrum takes form of the Lorentz lineshape [34], we calculate Q factor as  $Q = f_0/\Delta f$ , where  $f_0$  is the resonant frequency and  $\Delta f$  is FWHM. It is well known that the Q factor of any resonator is mainly affected by two kinds of losses. One is the energy dissipated in materials of the resonator - nonradiative loss, and the other one is the radiation loss which depends on the geometry of the structure. Total sum of the losses -  $\gamma$  can be extracted from the FWHM of the absorption peak as  $\text{FWHM} = 2\gamma = \Delta f$ . Until now, huge values of Q factors have been reported for chiral response of

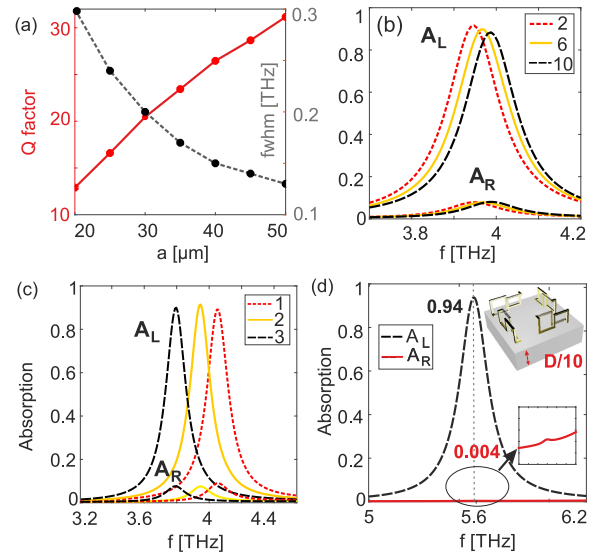


Fig. 5. (a) Q factor dependence on periodicity change (incident LCP wave). Impact of the variation of (b) the space in between each TCRR -  $r$  and (c) the cross-area thickness  $w$  on the absorption spectra ( $a = 40 \mu\text{m}$ ). (d) Absorption spectra for the case when the TCRRs structure is placed on the thin dielectric substrate and zoomed  $A_R$  spectra in the right corner ( $a = 40 \mu\text{m}$ ,  $D = 1.2 \mu\text{m}$ ). All quantities in legends are given in microns.

inverted metasurface consisting of an array of asymmetrically split ring apertures in microwave range [49], as well as of Si based structure at mid-IR frequencies [38]. In order to achieve more efficient circular polarization selective absorbers at THz frequencies, we focused on the calculation of the Q factor for different values of the geometrical parameters. In particular, here we analyze the change of Q factor and FWHM (Fig. 5(a)) with the variation of the period of the unit cell. Increase of Q factor and decrease of FWHM follow the increment of period size from 20 to 50  $\mu\text{m}$  (we are considering LCP wave). This indicates reduction of losses for larger values of period size. Having in mind that change of the period reflects geometrical changes of the structure, radiation losses should be dominantly influenced by the variation of period size [30], [50]. The maximum value

of  $Q = 31.2$  is achieved for  $a = 50 \mu\text{m}$  which is slightly larger than those obtained with the achiral THz structure based on split ring resonators [30].

Another geometric parameter we have examined is the distance  $r$  in between each TCRR inside the unit cell (Fig. 5(b)). The results imply a very slight change of the absorption with variation of  $r$  from 2 to  $10 \mu\text{m}$ . Similar results are obtained with the chiral metamaterial in ref. [27], where absorption coefficients of RCP and LCP waves were insignificantly changed by the variation of this parameter. Structures composed of few resonators in a unit cell exhibit two coupling mechanisms: intracoupling - in between resonators inside the unit cell, and intercoupling - due to interaction between unit cells [31]. The results indicate that intracoupling in between TCRRs in the unit cell is not disturbed with variation of  $r$  and consequently the overall absorption at the fundamental resonance remains unchanged. On the other hand, as it was seen in previous part of the paper, the intercoupling between unit cells was modified by the variation of  $a$  which affected the absorption magnitude and the performance of chiral metamaterial. Additionally, we investigate the influence of the width of the crossing area  $w$  on the absorption spectra (Fig. 5(c)). It is conclusive that this parameter has major influence on the resonance shift (change of about 0.3 THz to lower frequencies for increase of  $\Delta w = 1 \mu\text{m}$ ) and slightly modifies the absorption value. At the end, we examined the case in which our TCRRs structure is placed on the top of thin dielectric substrate with the thickness  $D/10$ . As it can be seen in Fig. 5(d), maximum value of absorption of LCP wave is 94%, while of RCP wave is almost negligible (the resonance exists but the maximum is very small - see the inset in the down-right corner at Fig. 5(d)) which indicates high CD value of 94%. If we compare this result with that presented in Fig. 2(b), we can conclude that the thickness of dielectric substrate has also significant influence on absorption value, as well as the period size. Although thicker substrates provide better mechanical support to metal resonators, the performance of the metamaterial is reduced. By placing TCRRs on a thin substrate, the absorption maximum of LCP wave is enhanced and of RCP one is significantly reduced which makes this kind of structure applicable for circular polarization selective components.

## V. SUMMARY

In this work we propose design of chiral metamaterial based on a unit cell with four rotated TCRRs embedded into dielectric material. Three resonant peaks into the absorption spectra are identified. The nature of these peaks is determined via analysis of electric field distributions and surface current flows. Analyzing the impact of geometric parameters variation on the metamaterial performances around the fundamental resonance, we showed that the main influence on absorption has variation of the structure period. For  $a = 40 \mu\text{m}$ , the maximum value of absorption peak of LCP wave was around 92.1%, while of RCP wave was 7.8%. At the same time, higher values of Q factor and the reduction of FWHM are achieved which implies decrease of losses with the increase of period. On the other hand, the distance variation in between resonators shows slight impact on absorption spectrum. In addition, we investigated the case when

the TCRRs structure is placed on the top of a thin dielectric substrate and even higher value of left circularly polarized absorption is obtained in this case - 94%. This indicates that the thickness of the dielectric substrate is also important parameter for achieving high absorption. To sum up, through this study we propose design of a chiral structure with a huge circular dichroism and near-unity polarization selective absorption which makes it a good candidate for realization of different THz components: detectors, sensors, filters.

## ACKNOWLEDGMENT

The research of G. Gligorić, P. P. Beličev and Lj. Hadžievski was funded by the Ministry of Education, Science and Technological Development of the Republic of Serbia. The research of D. B. Stojanović was funded by the Ministry of Education, Science and Technological Development of the Republic of Serbia and in part by NPRP11S-1126-170033 project of the Qatar National Research Fund (a member of the Qatar Foundation). The work of M. R. Belić was supported by NPRP11S-1126-170033 project of the Qatar National Research Fund. The work has been done in the context of Cost Action CA18223.

## REFERENCES

- [1] M. Tonouchi, "Cutting-edge terahertz technology," *Nature Photon.*, vol. 1, no. 2, pp. 97–105, Feb. 2007.
- [2] S. S. Dhillon *et al.*, "The 2017 terahertz science and technology roadmap," *J. Phys. D: Appl. Phys.*, vol. 50, no. 4, Jan. 2017, Art. no. 043001.
- [3] H. Zou and Y. Cheng, "A thermally tunable terahertz three-dimensional perfect metamaterial absorber for temperature sensing application," *Modern Phys. Lett. B*, vol. 34, no. 18, May 2020, Art. no. 2050207.
- [4] F. Chen, Y. Cheng, and H. Luo, "Temperature tunable narrow-band terahertz metasurface absorber based on insb micro-cylinder arrays for enhanced sensing application," *IEEE Access*, vol. 8, pp. 82 981–82 988, 2020.
- [5] H. Zou and Y. Cheng, "Design of a six-band terahertz metamaterial absorber for temperature sensing application," *Opt. Mater.*, vol. 88, pp. 674–679, Feb. 2019.
- [6] B.-X. Wang, X. Zhai, G.-Z. Wang, W.-Q. Huang, and L.-L. Wang, "A novel dual-band terahertz metamaterial absorber for a sensor application," *J. Appl. Phys.*, vol. 117, no. 1, Jan. 2015, Art. no. 014504.
- [7] I. Al-Naib, "Biomedical sensing with conductively coupled terahertz metamaterial resonators," *IEEE J. Sel. Topics Quantum Electron.*, vol. 23, no. 4, Jul./Aug. 2017, Art. no. 4700405.
- [8] W. Xu, L. Xie, and Y. Ying, "Mechanisms and applications of terahertz metamaterial sensing: a review," *Nanoscale*, vol. 9, no. 37, pp. 13 864–13 878, 2017.
- [9] W. Li and Y. Cheng, "Dual-band tunable terahertz perfect metamaterial absorber based on strontium titanate (STO) resonator structure," *Opt. Commun.*, vol. 462, p. 125265, May 2020.
- [10] N. I. Landy, S. Sajuyigbe, J. J. Mock, D. R. Smith, and W. J. Padilla, "Perfect metamaterial absorber," *Phys. Rev. Lett.*, vol. 100, no. 20, May 2008, Art. no. 207402.
- [11] C. M. Watts, X. Liu, and W. J. Padilla, "Metamaterial electromagnetic wave absorbers," *Adv. Mater.*, vol. 24, no. 23, pp. OP98–OP120, May 2012.
- [12] J. K. Gansel *et al.*, "Gold helix photonic metamaterial as broadband circular polarizer," *Sci.*, vol. 325, no. 5947, pp. 1513–1515, Aug. 2009.
- [13] D. Stojanović, J. Radovanović, and V. Milanović, "Delay times in a terahertz chiral metamaterial slab," *Phys. Rev. A*, vol. 94, no. 2, p. 23848, Aug. 2016.
- [14] B. Wang, T. Koschny, and C. M. Soukoulis, "Wide-angle and polarization-independent chiral metamaterial absorber," *Phys. Rev. B*, vol. 80, no. 3, p. 33108, Jul. 2009.
- [15] M. Kuwata-Gonokami *et al.*, "Giant optical activity in quasi-two-dimensional planar nanostructures," *Phys. Rev. Lett.*, vol. 95, no. 22, Nov. 2005, Art. no. 227401.
- [16] L. D. Barron, *Molecular Light Scattering Opt. Activity*. Cambridge, U.K.: Cambridge Univ. Press, Sep. 2004.

- [17] E. Philip, M. Z. Gungordu, S. Pal, P. Kung, and S. M. Kim, "Review on polarization selective terahertz metamaterials: from chiral metamaterials to stereometamaterials," *J. Infrared, Millimeter, Terahertz Waves*, vol. 38, no. 9, pp. 1047–1066, Jun. 2017.
- [18] S. J. Park, S. H. Cha, G. A. Shin, and Y. H. Ahn, "Sensing viruses using terahertz nano-gap metamaterials," *Biomed. Opt. Express*, vol. 8, no. 8, p. 3551, Jul. 2017.
- [19] T. Kan *et al.*, "Enantiomeric switching of chiral metamaterial for terahertz polarization modulation employing vertically deformable MEMS spirals," *Nature Commun.*, vol. 6, no. 1, p. 8422, Oct. 2015.
- [20] W. J. Choi, G. Cheng, Z. Huang, S. Zhang, T. B. Norris, and N. A. Kotov, "Terahertz circular dichroism spectroscopy of biomaterials enabled by kirigami polarization modulators," *Nature Mater.*, vol. 18, no. 8, pp. 820–826, Jul. 2019.
- [21] M. Li, L. Guo, J. Dong, and H. Yang, "An ultra-thin chiral metamaterial absorber with high selectivity for LCP and RCP waves," *J. Phys. D: Appl. Phys.*, vol. 47, no. 18, p. 185102, Apr. 2014.
- [22] Z. Wang, H. Jia, K. Yao, W. Cai, H. Chen, and Y. Liu, "Circular dichroism metamirrors with near-perfect extinction," *ACS Photon.*, vol. 3, no. 11, pp. 2096–2101, Oct. 2016.
- [23] W. Li, Z. J. Coppens, L. V. Besteiro, W. Wang, A. O. Govorov, and J. Valentine, "Circularly polarized light detection with hot electrons in chiral plasmonic metamaterials," *Nature Commun.*, vol. 6, no. 1, p. 8379, Sep. 2015.
- [24] X.-T. Kong, L. K. Khorashad, Z. Wang, and A. O. Govorov, "Photothermal circular dichroism induced by plasmon resonances in chiral metamaterial absorbers and bolometers," *Nano Letters*, vol. 18, no. 3, pp. 2001–2008, Feb. 2018.
- [25] B. Tang, Z. Li, E. Palacios, Z. Liu, S. Butun, and K. Aydin, "Chiral-selective plasmonic metasurface absorbers operating at visible frequencies," *IEEE Photon. Technol. Lett.*, vol. 29, no. 3, pp. 295–298, Feb. 2017.
- [26] N. Yogesh, T. Fu, F. Lan, and Z. Ouyang, "Far-infrared circular polarization and polarization filtering based on fermat's spiral chiral metamaterial," *IEEE Photon. J.*, vol. 7, no. 3, pp. 1–12, Jun. 2015.
- [27] Y. Cheng, H. Chen, J. Zhao, X. Mao, and Z. Cheng, "Chiral metamaterial absorber with high selectivity for terahertz circular polarization waves," *Opt. Mater. Express*, vol. 8, no. 5, p. 1399, Apr. 2018.
- [28] Y. K. Srivastava and R. Singh, "Impact of conductivity on lorentzian and fano resonant high-q THz metamaterials: Superconductor, metal and perfect electric conductor," *J. Appl. Phys.*, vol. 122, no. 18, p. 183104, Nov. 2017.
- [29] R. T. Ako, A. Upadhyay, W. Withayachumnankul, M. Bhaskaran, and S. Sriram, "Dielectrics for terahertz metasurfaces: Material selection and fabrication techniques," *Adv. Opt. Mater.*, vol. 8, no. 3, Sep. 2019, Art. no. 1900750.
- [30] R. Singh, C. Rockstuhl, and W. Zhang, "Strong influence of packing density in terahertz metamaterials," *Appl. Phys. Lett.*, vol. 97, no. 24, p. 241108, Dec. 2010.
- [31] L. Cong, Y. K. Srivastava, and R. Singh, "Inter and intra-metamolecular interaction enabled broadband high-efficiency polarization control in metasurfaces," *Appl. Phys. Lett.*, vol. 108, no. 1, Jan. 2016, Art. no. 011110.
- [32] Y. Cheng, F. Chen, and H. Luo, "Multi-band giant circular dichroism based on conjugated bilayer twisted-semicircle nanostructure at optical frequency," *Phys. Lett. A*, vol. 384, no. 19, p. 126398, Jul. 2020.
- [33] Y. Z. Cheng, M. L. Huang, H. R. Chen, Y. J. Zhou, X. S. Mao, and R. Z. Gong, "Influence of the geometry of a gammadian stereo-structure chiral metamaterial on optical properties," *J. Mod. Opt.*, vol. 64, no. 15, pp. 1487–1494, Feb. 2017.
- [34] C. Wu *et al.*, "Spectrally selective chiral silicon metasurfaces based on infrared fano resonances," *Nature Commun.*, vol. 5, no. 1, p. 3892, May 2014.
- [35] Z. Li, S. Butun, and K. Aydin, "Ultrannarrow band absorbers based on surface lattice resonances in nanostructured metal surfaces," *ACS Nano*, vol. 8, no. 8, pp. 8242–8248, Aug. 2014.
- [36] D. B. Stojanovi, P. P. Believ, G. Gligori, and L. Hadzievski, "Terahertz chiral metamaterial based on twisted closed ring resonators," *J. Phys. D: Appl. Phys.*, vol. 51, no. 4, Jan. 2018, Art. no. 045106.
- [37] G. Kenanakis *et al.*, "Flexible chiral metamaterials in the terahertz regime: a comparative study of various designs," *Opt. Mater. Express*, vol. 2, no. 12, p. 1702, Nov. 2012.
- [38] J. Wu *et al.*, "Chiral metafoils for terahertz broadband high-contrast flexible circular polarizers," *Phys. Rev. Appl.*, vol. 2, no. 1, p. 14005, Jul. 2014.
- [39] K. Fan, A. C. Strikwerda, H. Tao, X. Zhang, and R. D. Averitt, "Stand-up magnetic metamaterials at terahertz frequencies," *Opt. Express*, vol. 19, no. 13, p. 12619, Jun. 2011.
- [40] L. Maiolo *et al.*, "Quarter-wave plate metasurfaces on electromagnetically thin polyimide substrates," *Appl. Phys. Lett.*, vol. 115, no. 24, p. 241602, Dec. 2019.
- [41] R. Pan *et al.*, "Photon diagnostics at the FLASH THz beamline," *J. Synchrotron Radiat.*, vol. 26, no. 3, pp. 700–707, Apr. 2019.
- [42] P. D. Cunningham *et al.*, "Broadband terahertz characterization of the refractive index and absorption of some important polymeric and organic electro-optic materials," *J. Appl. Phys.*, vol. 109, no. 4, pp. 043 505–043 505–5, Feb. 2011.
- [43] K. Nielsen, H. K. Rasmussen, A. J. Adam, P. C. Planken, O. Bang, and P. U. Jepsen, "Bendable, low-loss topas fibers for the terahertz frequency range," *Opt. Express*, vol. 17, no. 10, p. 8592, May 2009.
- [44] Y. Zhang, Y. Feng, B. Zhu, J. Zhao, and T. Jiang, "Switchable quarter-wave plate with graphene based metamaterial for broadband terahertz wave manipulation," *Opt. Express*, vol. 23, no. 21, p. 27230, Oct. 2015.
- [45] A. Ferraro, D. C. Zografopoulos, R. Caputo, and R. Beccherelli, "Guided-mode resonant narrowband terahertz filtering by periodic metallic stripe and patch arrays on cyclo-olefin substrates," *Sci. Rep.*, vol. 8, no. 1, pp. 1–8, Nov. 2018.
- [46] G. V. Naik, V. M. Shalaev, and A. Boltasseva, "Alternative plasmonic materials: Beyond gold and silver," *Adv. Mater.*, vol. 25, no. 24, pp. 3264–3294, May 2013.
- [47] M. A. Ordal, R. J. Bell, R. W. Alexander, L. L. Long, and M. R. Query, "Optical properties of fourteen metals in the infrared and far infrared: Al, Co, Cu, Au, Fe, Pb, Mo, Ni, Pd, Pt, Ag, Ti, V, and W," *Appl. Opt.*, vol. 24, no. 24, p. 4493, Dec. 1985.
- [48] D. J. Cho, F. Wang, X. Zhang, and Y. R. Shen, "Contribution of the electric quadrupole resonance in optical metamaterials," *Phys. Rev. B*, vol. 78, no. 12, Sep. 2008, Art. no. 121101.
- [49] F. Wang, Z. Wang, and J. Shi, "Theoretical study of high-q fano resonance and extrinsic chirality in an ultrathin babinet-inverted metasurface," *J. Appl. Phys.*, vol. 116, no. 15, Oct. 2014, Art. no. 153506.
- [50] G. Isić, B. Vasić, D. C. Zografopoulos, R. Beccherelli, and R. Gajić, "Electrically tunable metalsemiconductor-metal terahertz metasurface modulators," *IEEE J. Sel. Top. Quantum Electron.*, vol. 25, no. 3, May 2019, Art. no. 8500108.

**Danka B. Stojanović** was born in Belgrade, Serbia, in 1987. She received the Diploma degree in physical electronics and the Ph.D. degree in nanoelectronics and photonics from the School of Electrical Engineering, University of Belgrade, Belgrade, Serbia, in 2011 and 2018, respectively. Her research interests include the fields of metasurfaces and metamaterials for diverse applications, ranging from light modulators and sensing at THz and IR frequencies, to structures in visible range applicable for solar cell technology.

**Goran Gligorić** was born in Loznica, Serbia, in 1979. He received the Ph.D. degree in electrical engineering from the School of Electrical Engineering, University in Belgrade, Belgrade, Serbia, in 2010. His research interests are in the field of physics of complex and ultra-cold systems, nonlinear optics and metamaterials.

**Petra P. Beličev** received the Ph.D. degree in electrical engineering from Belgrade University, Belgrade, Serbia, at the Group for Nanoelectronics, Optoelectronics and Laser Technique. She is a Senior Research Associate currently employed in the Institute of Nuclear Sciences Viñca in PSTAR Group. Her research interests include nonlinear optics, discrete solitons, metamaterials and fiber-optic sensors.

**Milivoj R. Belić** was born in Yugoslavia. He finished the School of Mathematics in Belgrade, Serbia in 1970. He received the B.S. degree in physics with the University of Belgrade, in 1974 and the Ph.D. degree in physics from the City College of New York, in 1980.

**Ljupčo Hadžievski** was born in Yugoslavia. He received the B.S. and M.S. degrees from the School of Electrical Engineering, University in Belgrade, Belgrade, Serbia and the Ph.D. degree at the Faculty of Physics, University in Belgrade. His research interests include are physics of complex and ultra-cold systems, nonlinear optics, discrete solitons, fiber-optic sensors and metamaterials.